# Site-Directed Incorporation of *p*-Nitrophenylalanine into Streptavidin and Site-to-Site Photoinduced Electron Transfer from a Pyrenyl Group to a Nitrophenyl Group on the Protein Framework

**Hiroshi Murakami, Takahiro Hohsaka, Yuki Ashizuka, and Masahiko Sisido***

*Contribution from the Department of Bioscience and Biotechnology, Faculty of Engineering, Okayama University, 3-1-1 Tsushimanaka, Okayama 700-8530, Japan*

*Received June 9, 1997*

**Abstract:** Site-directed mutagenesis of streptavidin was carried out using a frame-shift suppressor tRNA that is aminoacylated with L-*p*-nitrophenylalanine and has a CCCG 4-base anticodon. Streptavidins carrying a single *p*-nitrophenylalanine at 22 different sites were prepared from mRNAs that contain a single CGGG 4-base codon at the mutation site. Of the 22 mutants, 14 mutants were found to bind *N*-biotinyl-L-1-pyrenylalanine. Site-to-site photoinduced electron transfer from the excited pyrenyl group to the nitrophenyl group was observed with steady-state fluorescence spectroscopy as well as by fluorescence decay measurement. The rate constants of the electron transfer decreased with the edge-to-edge distances that were predicted from the X-ray crystallographic structure of streptavidin. The distance dependence was analyzed on the basis of the tunneling pathway model. It was found that the rate constants are compatible with those in other proteins carrying metal complexes, except for the cases where electron transfer occurs through long space.

Site-directed incorporation of nonnatural amino acids is a versatile technique through which a variety of functional groups may be placed on the three-dimensional molecular framework of proteins. The technique first reported by Schultz's group[1] and Chamberlin's[2] group has been extended to incorporate a variety of nonnatural amino acids[3−5] and to use 4-base codon−anticodon pairs for addressing nonnatural amino acids.[6]

One of the attractive goals of this technique is to build paths for electron transfer (ET) and energy transfer in proteins. Since these photoprocesses are very sensitive to the distances between donors and acceptors on the order of several angstroms, the site-specific incorporation of these groups into the three-dimensional molecular framework will be a powerful approach to achieve artificial photoenergy conversions and to design other photoelectronic devices. For this approach to be successful, however, one must have detailed information on the proper chromophore arrangements for effective ET in proteins.

Electron transfer in proteins has been attracting the interest of a number of researchers. In recent years, attention seems to be focused on the distance dependence of the ET rates. The ET rate constants in several different protein systems have been found to decay exponentially against the edge-to-edge distance between the donor and the acceptor, $\exp(-\beta r_{ee})$, with the distance decay constant $\beta$. Dutton and co-workers[7] proposed that the $\beta$ values for different protein systems seem to be roughly the same value, 1.4 $Å^{-1}$. Jay-Gerin and co-workers[8] reexamined the ET rates in various proteins and found that the distance decay constant for proteins excluding those of photosynthetic reaction centers is 0.66 $Å^{-1}$. However, Gray and co-workers made closer investigation of different protein systems that have different secondary and tertiary structures and found that the $\beta$ value may depend on the detailed molecular structure of the proteins.[9] This indicates that the electronic coupling, $H_{DA}$, between the donor and acceptor may depend on the intervening medium, that is, the conformation of the polypeptide chain and the mode of their connectivity.

Beratan et al.[10] proposed a tunneling pathway model in which the electronic coupling is calculated for a particular path along a sequence of $\sigma$ bonds with occasional jumps through space or through hydrogen bonds. If there are several possible pathways of comparable electronic coupling strengths, those must be summed up to obtain the total electronic coupling.[11] The

* Phone: +81-86-251-8218. Fax: +81-86-251-8219. E-mail: sisido@cc.okayama-u.ac.jp.

(1) Noren, C. J.; Anthony-Cahill, S. J.; Griffith, M. C.; Schultz, P. G. *Science* **1989**, *244*, 182.

(2) Bain, J. D.; Glabe, C. G.; Dix, T. A.; Chamberlin, A. R.; Diala, E. S. *J. Am. Chem. Soc.* **1989**, *111*, 8013.

(3) Hohsaka, T.; Sato, K.; Sisido, M.; Takai, K.; Yokoyama, S. *FEBS Lett*. **1994**, *344*, 171.

(4) Mamaev, S. V.; Laikhter, A. L.; Aslan, T.; Hecht, S. M. *J. Am. Chem. Soc*. **1996**, *118*, 7243.

(5) Steward, L. E.; Collins, C. S.; Gilmore, M. A.; Carlson, J. E.; Ross, J. B. A.; Chamberlin, A. R. *J. Am. Chem. Soc*. **1997**, *119*, 6.

(6) Hohsaka, T.; Ashizuka, Y.; Murakami, H.; Sisido, M. *J. Am. Chem. Soc*. **1996**, *118*, 9778.

(7) Moser, C. C.; Keske, J. M.; Warncke, K.; Farid, R. S.; Dutton, P. L. *Nature* **1992**, *355*, 796.

(8) Lopez-Castillo, J-.M.; Filali-Mouhim, A.; Nguyen, E.; Binh-Otten, V.; Jay-Gerin, J.-P. *J. Am. Chem. Soc.* **1997**, *119*, 1978.

(9) (a) Langen, R.; Colon, J. L.; Casimiro, D. R.; Karpishin, T. B.; Winkler, J. R.; Gray, H. B. *JBIC, J. Biol. Inorg. Chem.* **1996**, *1*, 221. (b) Gray, H. B.; Winkler, J. R. *Annu. Rev. Biochem*. **1996**, *65*, 537. (c) Wuttke, D. S.; Bjerrum, M. J.; Winkler, J. R.; Gray, H. B. *Science* **1992**, *256*, 1007. (d) Beratan, D. N.; Onuchic, J. N.; Winkler, J. R.; Gray, H. B. *Science* **1992**, *258*, 1740. (e) Wuttke, D. S.; Bjerrum, M. J.; Chang, I.-J.; Winkler, J. R.; Gray, H. B. *Biochim. Biophys. Acta* **1992**, *1101*, 168. (f) Casimiro, D. R.; Richards, J. H.; Winkler, J. R.; Gray, H. B. *J. Phys. Chem*. **1993**, *97*, 13073. (g) Langen, R.; Chang, I.-J.; Germanas, J. P.; Richards, J. H.; Winkler, J. R.; Gray, H. B. *Science* **1995**, *268*, 1733.

(10) (a) Beratan, D. N.; Onuchic, J. N.; Hopfield, J. J. *J. Chem. Phys*. **1987**, *86*, 4488. (b) Onuchic, J. N.; Beratan, D. N. *J. Chem. Phys*. **1990**, *92*, 722. (c) Beratan, D. N.; Betts, J. N. Onuchic, J. N. *Science* **1991**, *252*, 1285. (d) Beratan, D. N.; Betts, J. N.; Onuchic, J. N. *J. Phys. Chem*. **1992**, *96*, 2852.

S0002-7863(97)01890-8 CCC: $15.00 
Published on Web 07/11/1998

tunneling pathway model has been successfully applied to several protein systems carrying metal complexes.[9c−g,11,12]

For the study of the distance dependence of ET, the donors and acceptors must be placed at a variety of sites in the same protein, and for this purpose, the technique of site-directed incorporation of nonnatural amino acids will play an essential role. Incorporation of bipyridylalanine into cytochrome *c* has been reported by Gray and Imperiali[13] through a semisynthetic mutation. This technique is effective for incorporating a nonnatural amino acid at a particular position where the protein is chemically or enzymatically cleaved, but it is not a general method for placing a variety of chromophores at a number of different sites.

In this study, we have incorporated a single L-*p*-nitrophenylalanine (ntrPhe) into streptavidin at 22 different sites (22nd, 25th, 43rd, 44th, 49th, 51st, 52nd, 54th, 65th, 79th, 80th, 83rd, 84th, 85th, 87th, 92nd, 101st, 108th, 114th, 117th, 120th, and 124th). Also, a pyrenyl group was introduced to the protein by linking L-1-pyrenylalanine[14] to biotin (Bi−Py, structure I).

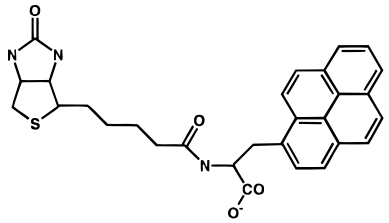

Biotin has been known to bind to streptavidin with an association constant on the order of $10^{15}$ $M^{-1}$. In this way, we have incorporated a pyrenyl group (P)−*p*-nitrophenyl group (T) pair into streptavidin with a variety of P−T distances and orientations.

A variety of model helical polypeptides that carry the P−T pair have been synthesized, and in these polypeptides, P works as a photosensitizer and T as an electron acceptor.[15] The photoinduced ET on the P−T pair in streptavidin has the following characteristic features as compared with those of other sensitizer−acceptor pairs that have been studied in proteins so far. (1) The excited state of P is a singlet state, and its intrinsic lifetime is relatively short (about 200 ns). (2) The excited state P* has a higher energy than those of porphyrins and metal porphyrins, and the high excited energy may cause possible electronic interactions with aromatic side groups in the proteins. (3) The sizes of P and T are relatively small, and this may reduce the possible ET paths.

## Experimental Section

**Preparation of $tRNA_{CCCG}^{ntrPhe}$.** A tRNA that carries a CCCG anticodon and is charged with a *p*-nitrophenylalanine at the 3′ terminal was prepared as reported before.[6] The base sequence of tRNA was designed according to the sequence of yeast $tRNA^{Phe}$, and a CCCG anticodon was inserted at the anticodon loop. The tRNA that lacks a CA dinucleotide unit at the 3′ end was synthesized from the template DNA with T7 RNA polymerase. The resulting $tRNA_{CCCG}(-CA)$ was then linked with the above *p*-nitrophenylalanyl pdCpA by T4 RNA ligase.

**Preparation of mRNA That Encodes a Streptavidin Carrying a T7 Tag at the N-Terminal and a $His_6$ Tag at the C-Terminal.** A synthetic gene for streptavidin was purchased from R&D Systems Europe, and a PCR mutagenesis was performed to replace, for example, TAT(Tyr83) by the 4-base codon CGGG. A plasmid (pGSH) was designed to contain a sequence of T7 promoter, a T7 tag, a streptavidin including a single CGGG 4-base codon, a $His_6$ tag, and a T7 terminator. The mRNA was synthesized *in vitro* by T7 RNA polymerase.

The mRNAs were designed to find stop codons if the CGGG 4-base codons were not translated by the frame-shift suppressor $tRNA_{CCCG}^{ntrPhe}$. This is exemplified in the following sequence: -$CGGG^{83}$-$CGU^{84}$-$AAU^{85}$-. If the CGGG 4-base codon was translated by the suppressor $tRNA_{CCCG}^{ntrPhe}$, the protein synthesis continues to the end. However, if the first three bases of the CGGG codon were translated by the endogenous $tRNA_{CCG}^{Arg}$, a termination codon UAA appears after a GCG codon. As a result, the full-length streptavidin is produced only if the CGGG codon is successfully translated to ntrPhe. Similar tricks have been installed in the total mRNA sequence that is available in the Supporting Information.

**Detection and Binding Ability of Mutant Streptavidins.** *In vitro* protein synthesis was performed with *Escherichia coli* S30 lysates (Promega). For analytical experiments, a 2 $\mu$L quantity of S30 lysates was used for each batch (10 $\mu$L). The reaction mixture was subjected to SDS-PAGE, and Western blot analysis was performed using anti-T7 tag antibody (Novagen) and alkaline phosphatase-labeled anti-mouse IgG (Promega). The binding ability of the mutant streptavidins against biotin was examined by dot blot analysis of the reaction mixture using a biotin-linked alkaline phosphatase (Zymed).

For fluorescence studies, a large-scale production of mutant streptavidin was carried out using 20 $\mu$L of S30 lysates for each batch (100 $\mu$L). The reaction mixture was put onto a Ni-NTA column (30 $\mu$L of the agarose gel, QIAGEN). Since only the full-length mutant proteins that contain ntrPhe carry the C-terminal $His_6$ tag, the Ni-NTA column selectively binds the full-length mutants. After the column was washed with a 50 mM imidazole solution (10 mL) to remove impurity components, the protein was eluted by washing the column with a 500 mM imidazole solution (105 $\mu$L). To avoid adsorption of the proteins to the cell wall, 0.01% poly(ethylene glycol) was added to the eluent.

**Pyrenylalanine-Linked Biotin (Bi−Py).** Biotinyl L-1-pyrenylalanine was synthesized as described previously.[14] The concentration of Bi−Py was determined from absorption spectrum by using $\epsilon_{345} = 3.7 \times 10^4$ $M^{-1}$ $cm^{-1}$ in PBS buffer (50 mM sodium phosphate, 300 mM NaCl, pH = 7.0).

**Fluorescence Measurement.** Fluorescence spectra were recorded on a Jasco FP777 instrument. The excitation wavelength was 328 nm. The slit width was 1.5 nm for the excitation and 10 nm for the emission. The solution of mutant streptavidin containing poly(ethylene glycol) as a stabilizing agent and imidazole as an eluting agent was equilibrated with argon gas. It must be noted that since commercial imidazole contained a highly fluorescent impurity it was purified by repeated recrystallization until the background of the fluorescence spectra became negligible.

A $10^{-8}$ M Bi−Py solution (1.0 mL) was put into a quartz cell capped with a rubber septum, and the solution was equilibrated with argon gas for 20 min. After measuring the fluorescence spectrum of Bi−Py, a 10-$\mu$L aliquot of mutant streptavidin solution was added and the mixture was gently shaken. After the mixture was allowed to stand for 5 min at 25 °C, the fluorescence spectrum was measured again. This cycle was repeated until the fluorescence intensity reached the final value. Since the concentration of the mutant in the mother solution is not known accurately, the fluorescence titration curve was compared with theoretical curves calculated for various concentrations of the mutant, for various binding constants against the Bi−Py molecule, and for various values of the ET efficiencies. During the fluorescence measurement, the concentration of Bi−Py was gradually decreased due to the successive addition of the mutant solution. The dilution effect was also taken into account in the calculation. The concentration, the binding constant, and the ET efficiency that gave the least-squares fit to the experimental curve were employed.

Fluorescence decay curves were measured on a Horiba NAES550 instrument equipped with a hydrogen discharge lamp (pulse width ≈

(11) Casimiro, D. R.; Wong, L.-L.; Colon, J. L.; Zewert, T. E.; Richards, J. H.; Chang, I.-J.; Winkler, J. R.; Gray, H. B. *J. Am. Chem. Soc*. **1993**, *115*, 1485.

(12) Farver, O.; Skov, L. K.; Young, S.; Bonander, N.; Karlsson, B. G.; Vaenngard, T.; Pecht, I. *J. Am. Chem. Soc*. **1997**, *119*, 5453.

(13) Wuttke, D. S.; Gray, H. B.; Fisher, S. L.; Imperiali, B. *J. Am. Chem. Soc*. **1993**, *115*, 8455.

(14) Kuragaki, M.; Sisido, M. *Bull. Chem. Soc. Jpn*. **1997**, *70*, 261.

(15) Sisido, M. *Adv. Photochem*. **1997**, *22*, 197.

2.5 ns) and a time-correlated single-photon counting detection system. The excitation wavelength was 328 ± 5 nm. The monomer or excimer emission was selectively taken out by a combination of glass filters. The experimental decay curves were reconvoluted by an iterative least-squares method to obtain the decay constants.

**Prediction of the Positions and Orientations of the *p*-Nitrophenyl Side Groups and Pyrenyl Group in the Mutant Streptavidins.** The positions and orientations of the *p*-nitrophenyl side groups in the mutants were predicted from molecular mechanics calculations. The X-ray crystallographic structure of streptavidin with a biotin in the binding site[16] was employed as the starting conformation. The software (PROCON) used has been developed by one of the authors (M.S.) and is an extended version of ECEPP[17] to include a variety of nonnatural amino acids and a prosthetic group that is bound to the binding site.[18] The program reads the original crystallographic data from the protein data bank and converts the Cartesian coordinates of skeletal atoms to the internal coordinates (bond lengths, bond angles, and rotational angles) for each amino acid unit. Hydrogen atoms were added to the skeletal atoms, the bond lengths and bond angles being taken from the ECEPP parameters.[17] The rotational angles of OH, SH, $NH_2$, and $NH_3^+$ groups were optimized to give a local minimum energy. A cutoff distance, $r_{cut}$, was given in the energy calculations, beyond which no interaction was taken into consideration.

First, the biotin group of Bi−Py was placed at the X-ray crystallographic position of the bound biotin[14] and the four rotational angles of the pyrenylalanine [$\phi$ (N−C$^\alpha$), $\psi$ (C$^\alpha$−C′), $\chi_1$ (C$^\alpha$−C$^\beta$), and $\chi_2$ (C$^\beta$−C$^\gamma$)] were rotated from 0° to 360° to find stable orientations. The amide bond that links the biotin and pyrenylalanine was assumed to take a planar trans form ($\omega$ = 180°).

The biotin moiety of the Bi−Py molecule was placed at the biotin binding site, and the pyrenylalanine unit was set to the most stable conformation. Then, one of the amino acids in streptavidin was replaced by a ntrPhe unit, and a side-chain energy contour map of the ntrPhe was drawn by varying $\chi_1$ (C$^\alpha$−C$^\beta$) and $\chi_2$ (C$^\beta$−C$^\gamma$). Starting from the energy minimum in the contour map, energy minimization was performed by varying the side-chain angles of the ntrPhe unit and those of the neighboring units whose side chains had an atom located closer than $r_{cut}$ to one of the side-chain atoms of the ntrPhe unit. The main chain was fixed to the original crystallographic structure; otherwise the protein will eventually become unfolded. If the pyrenylalanine unit of the Bi−Py was also close to the ntrPhe unit, the rotational angles of pyrenylalanine ($\phi$, $\psi$, $\chi_1$, and $\chi_2$) were also varied. Streptavidin is known to exist as a tetramer in solution. If the ntrPhe unit was close to some amino acids on another subunit of the tetramer, the side chains of the latter amino acids were also taken into consideration in the energy calculations.

The conformations were illustrated by using a personal computer version of NAMOD.[19] From the coordinates of the minimum-energy conformation, the closest aromatic carbon−aromatic carbon distance was obtained and used as the edge-to-edge distance $r_{ee}$ between the P and T groups.

## Results and Discussion

**Yields of Mutant Streptavidins and Their Binding Abilities against Biotin.** The yields of the mutant streptavidins were checked by Western blot analysis using alkaline phosphatase-linked anti-T7 antibody after SDS-PAGE analysis of the *in vitro* reaction mixture. The results for a variety of mutants that contain a single ntrPhe unit at different sites are shown in Figure 1.

The number of amino acids and the molecular weight of the streptavidin including the T7 tag and the $His_6$ tag are 180 and 19 000 respectively. The Western blots in Figure 1 indicates

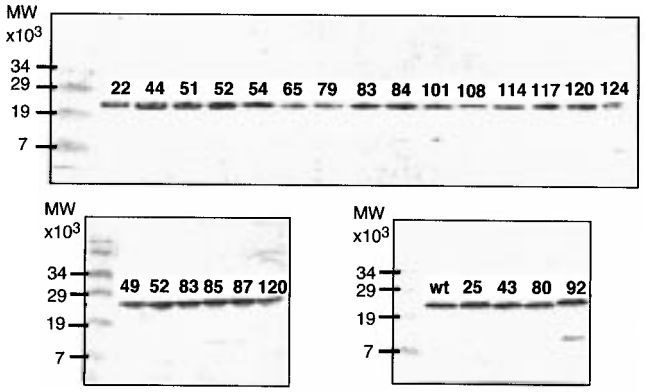


**Figure 1.** Results of Western blot analysis on the wild-type and the mutant streptavidins prepared in the S30 *in vitro* biosynthesizing system. The proteins were visualized with anti-T7 tag antibody combined with alkaline phosphatase-labeled anti-mouse IgG. The number on the top of each band indicates the mutation site.

that full-length streptavidins are produced in all cases. This indicates that a single ntrPhe unit is correctly incorporated into each protein; otherwise no full-length streptavidin would be produced. The yields of mutant streptavidins do not vary greatly for all mutants.

The binding abilities of the mutant streptavidins were checked by dot blotting of the *in vitro* reaction mixture, using biotin-labeled alkaline phosphatase as the marker. The results are shown in Figure 2. Although the yields of the mutant streptavidins were about the same, the blotting colors for the various mutants differ markedly, indicating that the binding abilities depend on the positions of the ntrPhe units. For example, the ntrPhe43, ntrPhe54, ntrPhe84, and ntrPhe120 mutants seem to keep the original binding ability, whereas the ntrPhe44, ntrPhe49, and ntrPhe87 mutants show little binding ability. It must be noted here that since the dot blot analysis is carried out under a very dilute condition of the biotin-labeled enzyme, even a trace of the color may show moderately strong binding against the biotin derivative.

The mutant streptavidins that showed even a small binding activity in the dot blot were prepared on a 100 $\mu$L scale of the S30 lysates and were purified with an Ni-NTA affinity column. The purity of the mutant streptavidin was checked by SDS-PAGE. The result is exemplified for the ntrPhe22, ntrPhe51, ntrPhe52, ntrPhe54, ntrPhe79, and ntrPhe83 mutants in Figure 3. The purification procedure using the His6/Ni-NTA system is good enough for the following experiments.

**Fluorescence Behavior of Biotin-Linked Pyrenylalanine That Is Bound to a Tetramer of Native and Wild-Type Streptavidin.** Before discussing photoinduced electron transfer, the photophysical property of biotin-linked pyrenylalanine (Bi−Py) that is bound to a tetramer of wild-type or native streptavidin was studied. The wild-type streptavidin is a protein that was prepared through *in vitro* synthesis without mutation and has a T7 tag at the N-terminal and a $His_6$ tag at the C-terminal. Figure 4a shows the fluorescence spectra of $10^{-8}$ M Bi−Py in the presence of different amounts of the wild-type streptavidin. The pyrenyl fluorescence decreased with the addition of streptavidin, and the decrease stopped after almost all Bi−Py molecules were bound to the streptavidin. With the decrease of monomer emission, a small and broad fluorescence band appeared around 500 nm. Similar behavior was observed when native streptavidin was used. When further native streptavidin was added to the solution to give a protein:Bi−Py ratio of 16:1, the 500-nm emission decreased again and the intensity of monomer

(16) Weber, P. C.; Ohlendorf, D. H.; Wendoloski, J. J.; Salemme, F. R. *Science* **1989**, *243*, 85.
(17) Momany, F. A.; McGuire, R. F.; Burgess, A. W.; Scheraga, H. A. *J. Phys. Chem.* **1975**, *79*, 2361.
(18) (a) Sisido, M. *Pept. Chem.* **1992**, *29*, 105. (b) Sisido, M.; Beppu, Y. *Japan Chemistry Program Exchange (JCPE)* No. P057.
(19) Beppu, Y. *Comput. Chem.* **1989**, *13*, 101.

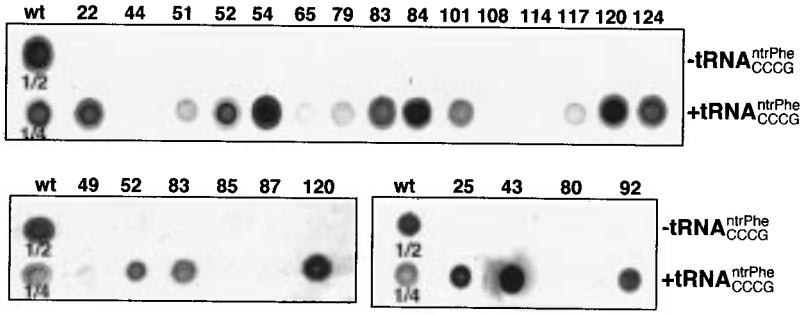


**Figure 2.** Results of dot blot analysis for the wild-type and the mutant streptavidins. The binding abilities are visualized with a biotin-labeled alkaline phosphatase. No mutant is formed in the absence of $tRNA_{CCCG}^{ntrPhe}$. The wild-type streptavidin was obtained in the absence of the tRNA.

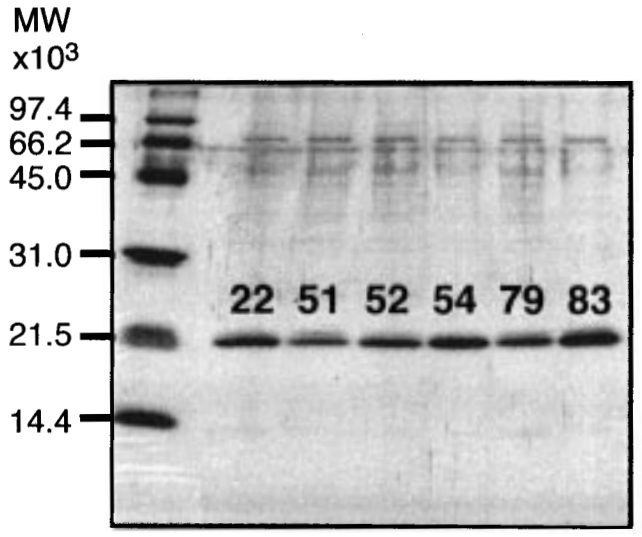


**Figure 3.** Results of SDS-PAGE analysis for purified mutants through a $His_6$/Ni-NTA affinity column. The proteins were visualized with silver nitrate.

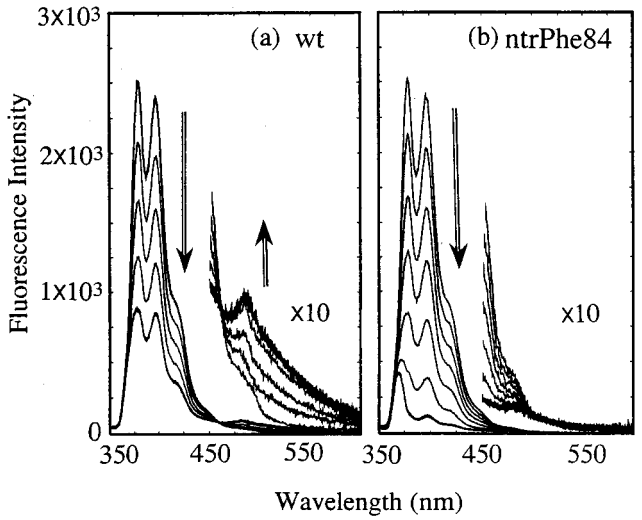


**Figure 4.** Fluorescence spectra of Bi−Py in the presence of different amounts of wild-type streptavidin (a) or ntrPhe84 mutant (b). [Bi−Py] $= 1 \times 10^{-8}$ M, $\lambda_{ex} = 328$ nm, 25 °C, under an argon atmosphere. The excimer band (450−600 nm) is magnified 10×.

fluorescence recovered up to 90% of the original value. The recovery of monomer fluorescence under an excess of streptavidin indicates that the 500-nm emission originates from a pyrenyl−pyrenyl interaction on the tetramer that is most effective when the protein:Bi−Py ratio is 1:1. Therefore, the broad emission is assigned to excimers that are formed in the tetrameric form of the streptavidins. The excimer fluorescence markedly decreased when the temperature was lowered to 5 °C, indicating that the excimer is formed after thermal fluctuations in the tetrameric protein and the fluctuations in the Bi−Py molecules inside the biding sites.

The orientation of the pyrenyl group in the tetramer was investigated through conformational energy calculations by rotating the N−$C^\alpha$ ($\phi$), $C^\alpha$−C′ ($\psi$), $C^\alpha$−$C^\beta$ ($\chi_1$), and $C^\beta$−$C^\gamma$ ($\chi_2$) bonds of the pyrenylalanine unit. Two possible low-energy orientations were found. Starting from these two local minima, energy minimizations were carried out by varying the rotational angles of the pyrenylalanine unit as well as those of the side chains of the protein. The minimum energy orientations with the optimized side-chain orientations of the protein were found at $\phi$, $\psi$, $\chi_1$, $\chi_2$ = 136°, 149°, 164°, 77° (type M) and 136°, 149°, 165°, 215° (type E). The two orientations differ only in the rotational angle of $\chi_2$, by 138°. In the type M orientation, the center-to-center distance between the closest pyrenyl groups in the tetramer was 13.3 Å and the edge-to-edge distance was 8.7 Å. These distances are too far to form excimers even after large thermal fluctuations. In the type E orientation, the closest pyrenyl groups are separated by a center-to-center distance of 10.2 Å and by an edge-to-edge distance of 1.9 Å. These distances are short enough to form excimers after small thermal motions of the pyrenyl groups. The conformational energy of the type E orientation was higher than that of the type M orientation by 21 kcal $mol^{-1}$. The tetramer conformation with Bi−Py molecules in the type E orientation is illustrated in Figure 5. The two pyrenyl groups are very close to each other but are arranged in the head-to-head configuration, which is not appropriate to form normal sandwich-type excimers.

In the fluorescence spectra of Figure 4a, the intensity of the excimer fluorescence is very small compared with the large decrease of monomer fluorescence, suggesting that the two pyrenyl groups easily come close to each other but do not form normal sandwich-type excimers. The spectroscopic finding is consistent with the tetrameric conformation in Figure 5. Therefore, we assume that the pyrenyl groups are in the type E orientation, although a somewhat higher conformational energy has been predicted. The higher energy may be compensated for, at least partly, by taking the flexibility of the main-chain conformation into account.

Fluorescence rise and decay curves were measured for the monomer and excimer emission in the presence of an equal molar amount of native streptavidin. The monomer decay curve could be fitted to a three-component exponential function with $\tau_1 = 8.0$ (0.024), $\tau_2 = 40.4$ (0.272), and $\tau_3 = 114.4$ (0.703) [ns (weighting factor)] ($\chi^2 = 1.09$). The excimer curve was analyzed with $\tau_1 = 8.1$ (−0.028), $\tau_2 = 67.9$ (0.647), and $\tau_3 = 98.1$ (0.357) ($\chi^2 = 1.12$). The rise component of the excimer with $\tau_1 = 8.1$ indicates that the excimer is formed through

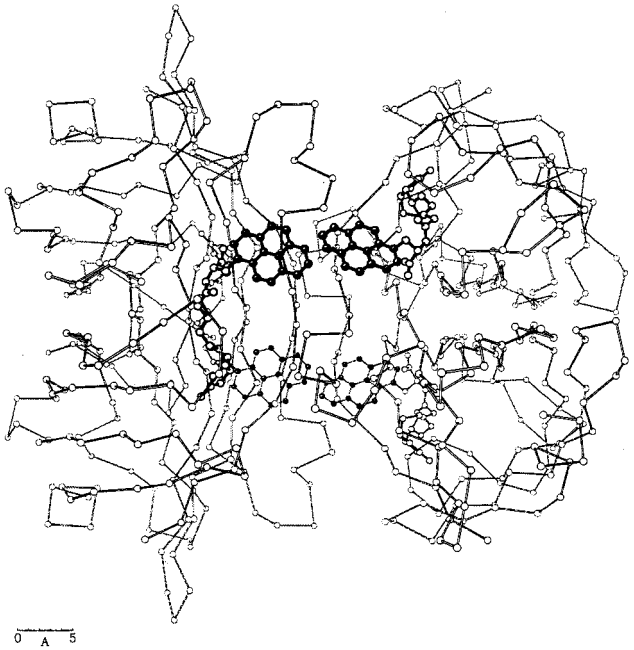


**Figure 5.** The tetramer conformation of native streptavidin with four Bi−Py molecules in the binding sites of biotin. The biotin group of the Bi−Py is fixed to the X-ray crystallographic position of biotin and the pyrenylalanine unit is in the type E orientation. $\omega$ (C′−N), $\phi$ (N−C$^{\alpha}$), $\psi$ (C$^{\alpha}$−C′), $\chi_1$ (C$^{\alpha}$−C$^{\beta}$), $\chi_2$ (C$^{\beta}$−C$^{\gamma}$) = 180°, 136°, 149°, 165°, and 215°, respectively.

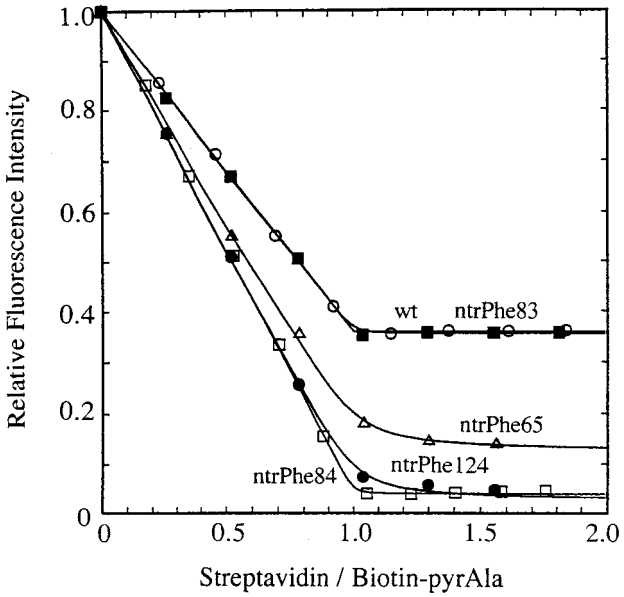


**Figure 6.** Relative fluorescence intensity of $10^{-8}$ M Bi−Py in the presence of different amounts of wild-type streptavidin (solid squares), ntrPhe83 (open circles), ntrPhe65 (open triangles), ntrPhe84 (open squares), and ntrPhe124 (solid circles) mutants. $\lambda_{em}$ = 397 nm, $\lambda_{ex}$ = 328 nm, 25 °C, under an argon atmosphere. Solid lines are the best-fit curves obtained by varying the concentration of the mother solution of each protein, the binding constant against the Bi−Py molecule, and the ET efficiency.

thermal fluctuations of the tetrameric protein and the rotational motion of the pyrenylalanine unit to attain the emissive excimer conformation starting from the type E conformation in Figure 5. However, since the weighting factor of the rise component is much smaller than that of the decay component, the presence of a preformed excimer is also indicated.

**Fluorescence Quenching of Biotin-Linked Pyrenylalanine by Mutant Streptavidins Carrying Single *p*-Nitrophenylalanine.** The fluorescence spectra of Bi−Py in the presence of different amounts of the mutant streptavidin carrying single ntrPhe at the 84th site are shown in Figure 4b. The decrease of monomer fluorescence with the addition of the mutant is more marked, and the final fluorescence intensity is much smaller than those observed with the wild-type streptavidin. The behavior in the presence of the ntrPhe84 mutant is attributed to a photoinduced electron transfer from the excited P group to the T group, as has been studied in model polypeptide systems that contain the P−T pair.[15]

The fluorescence intensities are plotted against the protein: Bi−Py ratio for the wild-type, ntrPhe65, ntrPhe83, ntrPhe84, and ntrPhe124 streptavidins in Figure 6. Since concentrations of the proteins are not known accurately, a least-squares analysis was made for the experimental points. In the least-squares analysis, the concentration of the mother solution of each mutant, the binding constant of the mutant against the Bi−Py molecule, and the ET efficiency were optimized to find the best fit to the experimental points. The experimental points in Figure 6 are plotted against the best-fit values of the concentrations, and the solid lines are the calculated curves using the best-fit values of the binding constants and the ET efficiencies.

The binding constants for the ntrPhe83 and ntrPhe84 mutants are roughly the same as that of the wild-type protein ($K > 10^{11}$ $M^{-1}$), but those of the ntrPhe65 and ntrPhe124 mutants were $4.8 \times 10^{10}$ and $1.7 \times 10^{10}$ $M^{-1}$, respectively, indicating that the binding is more or less blocked by the incorporation of the ntrPhe unit. The binding constants for the all mutants are listed in Table 1.

The Bi−Py molecule that had been bound to the mutant streptavidins was released when a $10^4$-fold excess of biotin was added to the solution. Figure 7 shows the recovery of fluorescence intensity of Bi−Py after the addition of the excess amount of biotin to the solution of protein:Bi−Py ≈ 2:1. The recovery was very fast for the ntrPhe92 mutant and moderately fast for the ntrPhe84. The recovery was much slower for the ntrPhe65, ntrPhe83, and wild-type streptavidins. The recovery was found to follow first-order kinetics, and the first-order rate constants $k_{off}$ are listed in Table 1.

The release of the Bi−Py molecule by the addition of biotin indicates that the Bi−Py molecule is bound to the biotin binding site and competes with the biotin that was added. Judging from the slow recovery that is on the order of seconds or longer, we may assume that the Bi−Py molecule is staying in the binding site during the ET process that occurs within a few 10 nanoseconds or shorter.

**Rates of Photoinduced Electron Transfer in Mutant Streptavidins.** From the final fluorescence intensities of the wild-type and the mutant proteins in Figure 6, the efficiencies of ET from P* to T ($E_{ET}$) were calculated and are listed in Table 1. The efficiency is very sensitive to the position of the ntrPhe unit. For example, the efficiency for the ntrPhe83 mutant is virtually zero, whereas that for the ntrPhe84 mutant is 89%. The marked sensitivity to the position of the ntrPhe group indicates that the ET rate depends very sharply on distance and that the fluctuations of the main chain and the side chains are not so significant as to average out the difference in the positions of the ntrPhe83 and ntrPhe84 units.

The positions and orientations of the ntrPhe units on mutant streptavidins that are binding a Bi−Py molecule in their biotin binding site were predicted from molecular mechanics calculations. The starting conformation was taken from the X-ray

**Table 1.** Binding Constant against Bi−Py ($K$, $M^{-1}$), the First-Order Release Rate Constant of Bi−Py ($k_{off}$, $s^{-1}$), the Edge-to-edge Distance between P and T Groups in the Optimized Structure ($r_{ee}$, Å), the Efficiency of Electron Transfer ($E_{ET}$), the Rate Constant of Electron Transfer Evaluated from Fluorescence Intensity ($k_{ET}$, $s^{-1}$), and That from Average Fluorescence Decay Time ($k_{ET}$, $s^{-1}$), the Equivalent $\sigma$ Distance along the Optimum ET Pathway ($\sigma_L$(opt), Å), and the Equivalent $\sigma$ Distance for the Sum of the Possible ET Pathways ($\sigma_L$(sum), Å)

| mutation site | $K$ ($M^{-1}$) | $k_{off}$ ($s^{-1}$) | $r_{ee}$ (Å) | $E_{ET}$ | $k_{ET}$ inten ($s^{-1}$) | $k_{ET}$ decay ($s^{-1}$) | $\sigma_L$ (opt) (Å) | $\sigma_L$ (sum) (Å) |
|---|---|---|---|---|---|---|---|---|
| 22 | $>10^{11}$ | $<10^{-5}$ | 20.9 | <0.1 | $<1 \times 10^6$ | | 40.2 | 33.6 |
| 25 | $>10^{11}$ | $7.4 \times 10^{-5}$ | 12.4 | 0.72 | $3.8 \times 10^7$ | | 32.7 | 24.4 |
| 51 | $6.9 \times 10^{10}$ | $<10^{-5}$ | 14.8 | <0.1 | $1.8 \times 10^6$ | | 29.6 | 21.7 |
| 52 | $>10^{11}$ | $1.1 \times 10^{-5}$ | 18.1 | <0.1 | $<1 \times 10^6$ | | 33.8 | 26.3 |
| 54 | $>10^{11}$ | $3.7 \times 10^{-4}$ | 11.3 | 0.74 | $3.8 \times 10^7$ | $4.3 \times 10^7$ | 34.7 | 21.7 |
| 65 | $4.8 \times 10^{10}$ | $<10^{-5}$ | 38.1<br>9.3(4th) | 0.63 | $2.6 \times 10^7$ | | 41.0 | 41.0 |
| 80 | $4.3 \times 10^{10}$ | $<10^{-5}$ | 13.1 | <0.1 | $<1 \times 10^6$ | | 28.2 | 19.7 |
| 83 | $>10^{11}$ | $<10^{-5}$ | 16.8 | <0.1 | $<1 \times 10^6$ | $1.8 \times 10^6$ | 34.6 | 29.0 |
| 84 | $>10^{11}$ | $1.0 \times 10^{-4}$ | 9.1 | 0.89 | $1.1 \times 10^8$ | | 30.5 | 28.6 |
| 92 | $1.1 \times 10^{10}$ | $4.5 \times 10^{-3}$ | 13.1 | 0.25 | $5.8 \times 10^6$ | $7.8 \times 10^6$ | 30.7 | 23.1 |
| 101 | $7.0 \times 10^{10}$ | $<10^{-5}$ | 28.7<br>24.3(4th) | <0.1 | $<1 \times 10^6$ | | 83.5 | 74.6 |
| 117 | $>10^{11}$ | $1.0 \times 10^{-5}$ | 12.3<br>10.6(3rd) | 0.76 | $4.7 \times 10^7$ | | 39.6 | 37.0 |
| 120 | $6.6 \times 10^9$ | $1.9 \times 10^{-4}$ | 9.9<br>5.9(3rd) | 0.90 | $1.3 \times 10^8$ | | 21.1 | 21.1 |
| 124 | $1.7 \times 10^{10}$ | $3.0 \times 10^{-5}$ | 4.7 | 0.95 | $2.6 \times 10^8$ | | 14.2 | 14.1 |
| w.t. | $>10^{11}$ | $<10^{-5}$ | | | | | | |

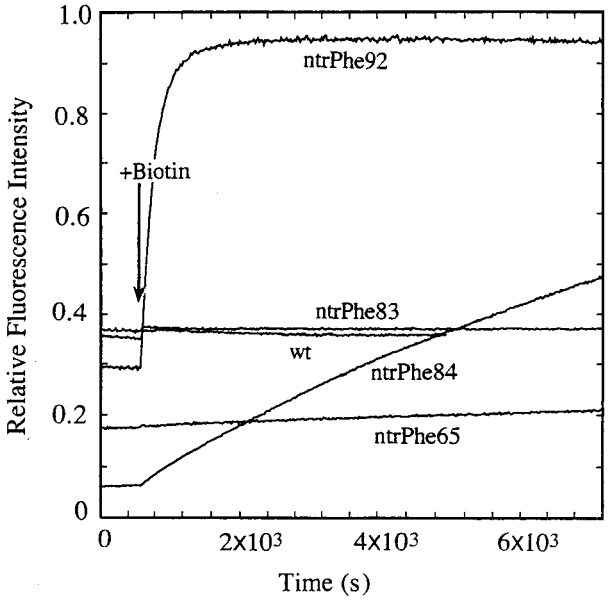


**Figure 7.** Recovery of fluorescence intensity of $10^{-8}$ M Bi−Py after adding $10^4$-fold excess of biotin to each mixture of protein:Bi−Py ≈ 2:1.

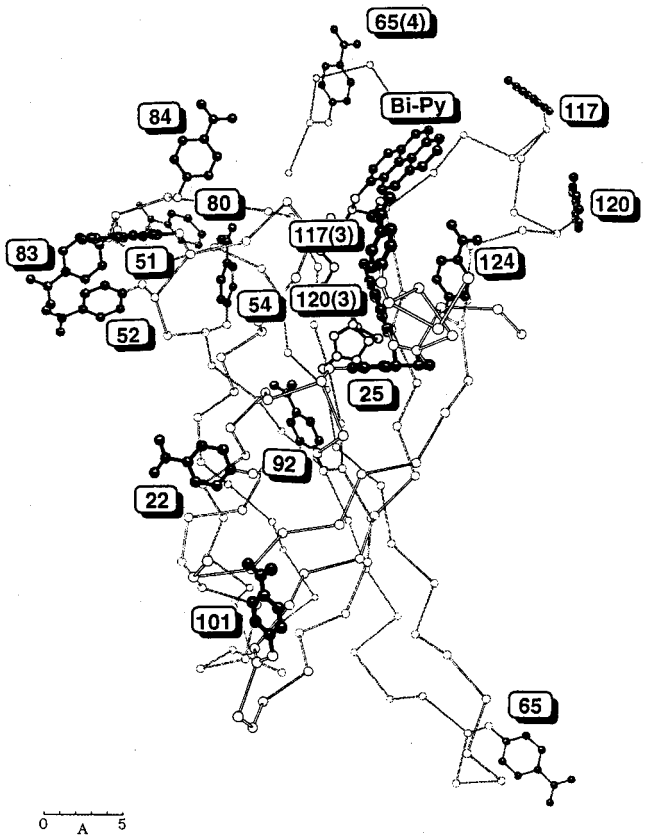


**Figure 8.** Computer-predicted orientation of nitrophenyl group in the mutants. Orientation of each ntrPhe unit is optimized by varying the side-chain angles of the ntrPhe unit and those of the neighboring amino acids that are located within $r_{cut}$ = 8 Å from the ntrPhe unit. If the Bi−Py molecule is also closer than 8 Å, the orientation of pyrenylalanine is also optimized for each mutant. In this figure the pyrenylalanine unit is set to the type E orientation in the native streptavidin.

crystallographic structure of native streptavidin with a biotin in its binding site.[16] The energy minimization was made by varying only the side groups of the ntrPhe unit and of the neighboring amino acids that are located within $r_{cut}$ = 8 Å from the ntrPhe unit. The computer-predicted orientations of the ntrPhe units at the 14 different sites are illustrated in Figure 8, together with the Bi−Py molecule in the type E orientation; $\phi$, $\psi$, $\chi_1$, and $\chi_2$ = 136°, 149°, 165°, and 215°, respectively. It must be noted that the orientation of the P group differs slightly with the positions and orientations of the ntrPhe unit. The orientation shown in Figure 8 is that for the wild-type protein and does not correspond accurately to the P−T distances that will be discussed below.

The difference of ET efficiencies for different mutants may be interpreted simply in terms of the difference of the edge-to-edge distances between the P and T groups. For example, the very different efficiencies of the ntrPhe83 and ntrPhe84 mutants may be explained in terms of the orientation of the ntrPhe unit at the two sites. As shown in Figure 8, the ntrPhe83 unit is oriented in the opposite direction to that of the P group ($r_{ee}$ = 16.8 Å), due mainly to the constraints of the main-chain conformation and a steric repulsion with Glu51. On the other hand, the ntrPhe84 unit is oriented toward the P group ($r_{ee}$ = 9.1 Å) due to the main-chain constraints.

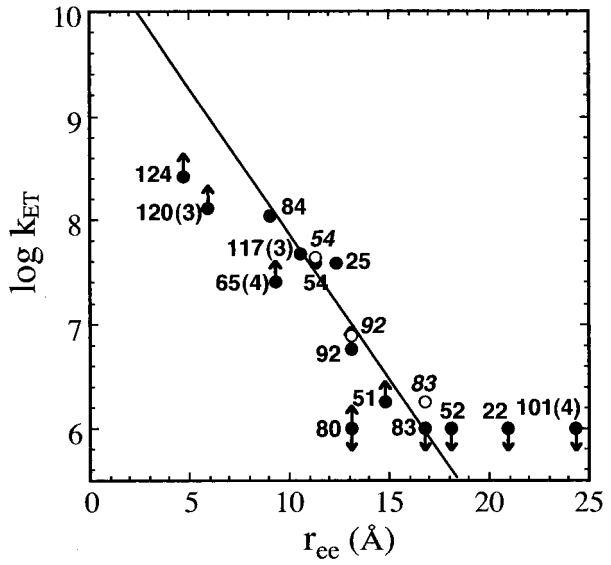


**Figure 9.** Rate constants of electron transfer from the pyrenyl group of the Bi−Py molecule to the nitrophenyl group at several different sites evaluated from the quenching of fluorescence intensity (solid circles) or from the average fluorescence lifetime (open circles). The abscissa is the closest edge-to-edge distance between the pyrenyl and nitrophenyl groups in the optimized tetramer conformation of each mutant. The points with downward arrows indicate that the ET rate was lower than $10^{-6}$ $s^{-1}$. The points with upward arrows indicate that the ET rate may be underestimated due to a lower binding constant against Bi−Py.

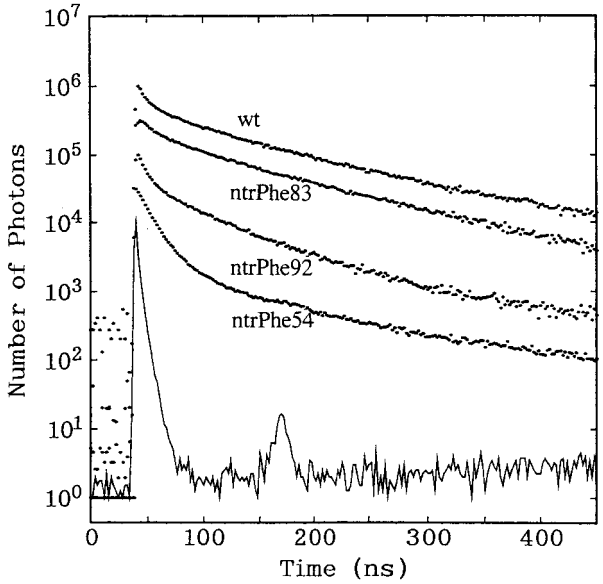


**Figure 10.** Fluorescence decay curves of the Bi−Py molecule in the presence of an equal amount of wild-type streptavidin or the ntrPhe mutant. Due to the small fluorescence intensity, the original decay curves contained a large scattering component in the early stage. The contribution of this component was evaluated by the least-squares analysis and has been subtracted from the original decay curves.

The ET to ntrPhe65 was moderately efficient (63%), but the latter is far separated from the P group ($r_{ee}$ = 38.1 Å) on the same subunit. The question may be solved by taking the tetramer structure into consideration. The ntrPhe65 unit in the fourth subunit was found to be close to the P group in the first unit ($r_{ee}$ = 9.3 Å), shown as ntrPhe65(4) in Figure 8. Judging from these facts, we have confirmed that the ntrPhe units are correctly incorporated into the right positions in the three-dimensional structure of streptavidin and that the ET efficiencies are determined by the distances in the tetrameric proteins. The closest edge-to-edge distance between the aromatic carbons in the pyrenyl and the nitrophenyl group are listed in Table 1.

The ET rate constant $k_{ET}$ may be obtained from the ET efficiency $E_{ET}$ and the average lifetime of P* bound to the wild-type streptavidin ($\langle\tau\rangle_0$):

$$k_{ET} = \langle\tau\rangle_0^{-1}\frac{E_{ET}}{(1-E_{ET})} = \langle\tau\rangle_0^{-1}\left(\frac{I_M(\text{wild-type})}{I_M(\text{mutant})} - 1\right) \quad (1)$$

where $I_M$(wild-type) and $I_M$(mutant) are the intensities of the monomer fluorescence of the pyrenyl group in the presence of the wild-type and mutant streptavidins, respectively. The fluorescence decay of the monomer fluorescence P* in the presence of an equal molar amount of the wild-type streptavidin followed two-component kinetics with $\tau_1$ = 27 ns (weight = 0.163) and $\tau_2$ = 108 ns (0.837), and the average lifetime $\langle\tau\rangle_0$ was 72.1 ns.[20]

The rate constants were calculated from the fluorescence intensities, and their logarithms were plotted against the closest edge-to-edge distances between the P and T groups (Figure 8, Table 1). The results are shown in Figure 9. Since the differences between the fluorescence intensities for the wild-type streptavidin and the mutants become very small when the ET rate constant becomes very small, the rate constant could be evaluated only down to the order of $10^6$ $s^{-1}$. The points for the ntrPhe22, ntrPhe51, ntrPhe52, ntrPhe80, ntrPhe83 (solid circle), and ntrPhe101 mutants in Figure 9 show only that they are less than $10^6$ $s^{-1}$.

Alternatively, the ET rate constants can be obtained from the decay kinetics. Since the fluorescence intensity was very weak due to low concentrations of the mutant proteins on the order of $10^{-8}$ M, the decay curve could be measured only for the mutants that show low ET efficiencies. The decay curves after subtracting a large scattering component are shown in Figure 10 for the wild-type and the ntrPhe83, ntrPhe92, and ntrPhe54 mutants. Since the subtraction was not perfect, the decay curves contain some uncertainty during the early stage. The decay curves did not follow single-exponential kinetics, but a major decay component of the ntrPhe92 mutant was found to have a decay time of 23 ns and that of the ntrPhe54 mutant was 8.7 ns. The average decay times $\langle\tau\rangle$ were calculated for the three mutants, and the ET rate constants were obtained from eq 2.

$$k_{ET} = \langle\tau\rangle^{-1} - \langle\tau\rangle_0^{-1} \quad (2)$$

The rate constants from the decay kinetics were also plotted in Figure 9 as open circles. The rate constants from the fluorescence intensities and from the decay times show reasonable agreement with each other for the ntrPhe54 and ntrPhe92 mutants, indicating that the ET observed in the present system is primarily a dynamic process in which an electron jumps from an excited P group to a T group that are spatially separated by the protein framework.

The deviation from the exponential decay kinetics indicates that the P and T groups are not fixed on single positions and their edge-to-edge distances are distributed over some range. Since the rate constants that can be measured in the P*−T system are on the order of $10^8$−$10^6$ $s^{-1}$, some of the modes of the polypeptide fluctuations including intersubunit motions may

(20) Since the amount of the wild-type streptavidin is on the order of $10^{-8}$ M and the decay curve contained a large scattering component in the early stage of the decay, the fast decay component due to excimer formation that was observed for the native streptavidin could not be detected.

be slower than the ET process. This may be the reason for the nonexponential decay of the fluorescence intensity.

The rate constants for the ntrPhe124, ntrPhe120, ntrPhe65, and ntrPhe80 mutants seem to be smaller than the values expected from other points. As shown in Table 1, these mutants show smaller binding constants against the Bi−Py molecule than the wild-type streptavidin ($>10^{11}$ $M^{-1}$). The smaller binding constant may cause incomplete binding of the Bi−Py molecule and results in smaller excimer quenching. Therefore, the observed ET rate constants of the four mutants are showing the lower limit. From the rest of the data points, the distance dependence of $k_{ET}$ may be roughly expressed by the exponential function $k_{ET0}\exp[-\beta(r_{ee} - 3)]$ with $k_{ET0} = 6.5 \times 10^9$ ($s^{-1}$) and $\beta = 0.63$ ($Å^{-1}$).

**Distance Dependence of Electron Transfer in Streptavidins.** The distance dependence of the ET rate constants in various proteins has been discussed extensively.[7−10] So far, however, only a few systematic studies have been reported in which a sensitizer−acceptor pair is distributed over a wide variety of sites in the same protein.[9] In the present ET system, the T group as an acceptor is distributed at a variety of sites in streptavidin, which allows us to discuss the distance dependence of ET in a single protein.

The distance dependence is most simply discussed under conditions where the ET is optimized for its Franck−Condon factor. The $\Delta G$ values for the P*−T pairs in mutant streptavidins are, however, very difficult to measure experimentally. If we assume the effective dielectric constant in the protein environment to be between 7.6 (THF) and 36.7 (DMF) and use the oxidation potential of the P group in DMF (1.20 V vs SCE)[21] and the reduction potential of the T group in DMF (−1.10 V vs SCE),[22] the driving force is roughly estimated to be between 0.7 and 1.1 eV. In the above calculation, the Coulombic term ($e^2/4\pi\epsilon r_{cc}$) has been neglected because it is smaller than 0.1 eV when the center-to-center P−T distance is larger than 5 Å. Since the above range of the $\Delta G$ is near the reorganization energy in proteins,[7] we assume that the ET in the P*−T system in streptavidin is nearly optimized for the Franck−Condon factor. Indeed, in a separate experiment in which a variety of electron acceptors were linked to biotin and an anthryl group was introduced into a specific site of streptavidin, the rate of photoinduced ET from the excited anthryl group to the acceptors reached near maximum when a *p*-nitrophenyl group was used as the acceptor.[23] Since the oxidation potential and the excitation energy of the anthryl group are about the same as those of the pyrenyl group, the above preliminary results indicate that the ET from P* to T in streptavidin is also nearly optimized for the Franck−Condon factor. The above consideration ensures that the distance dependence of $k_{ET}$ in Figure 9 can be compared directly with other data that have been normalized for their Franck−Condon factor.

The ET rate constants are replotted together with those for other protein systems excluding photoreaction centers in Figure 11. Very roughly speaking, the present rate constants (solid circles) are a little larger than those for other proteins but smaller than those for the photoreaction centers. The $\beta$ value taken from the present data (0.63) is in reasonable agreement with the average $\beta$ value (0.66) for the protein systems excluding photoreaction centers.[7] However, in both cases, the rate constant

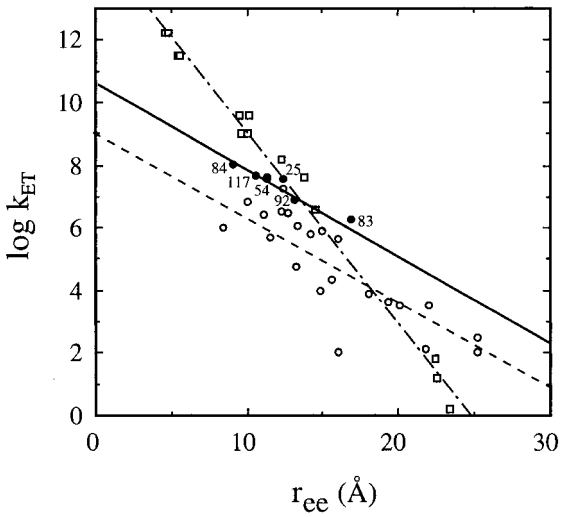


**Figure 11.** The ET rate constants in the present system (solid circles), in other protein systems excluding photoreaction centers (open circles, ref 10), and in photoreaction centers (open squares, ref 7) plotted against the edge-to-edge distance. The dashed lines indicate the exponential decay function with $\beta = 1.4$ (photoreaction centers), 0.63 (present system), and 0.66 (other protein systems), respectively.

extrapolated to the closest contact ($r_{ee} = 3$ Å) is much less than the value expected for the optimized Franck−Condon factor ($k_{ET0} = 10^{13}$ $s^{-1}$). This discrepancy indicates that the distance dependence in Figures 9 and 11 must be reexamined on the basis of a more sophisticated theory that takes the detailed molecular structure of protein into account.

**Analysis of the ET Rates on the Basis of the Tunneling Pathway Model.** The tunneling pathway model for ET in proteins has been proposed by Beratan et al.[10] and it has been successfully applied to several protein systems.[9] In this model, the matrix element of the protein-mediated electronic coupling is calculated as the product of the successive coupling terms along an ET pathway:

$$H_{DA} = \Pi_i \epsilon_C(i) \Pi_j \epsilon_S(j) \Pi_k \epsilon_H(k) \tag{3}$$

where $\epsilon_C(i)$, $\epsilon_S(j)$, and $\epsilon_H(k)$ are the coupling terms for ET along the *i*th $\sigma$-bond, for the *j*th through-space jump, and for the *k*th through-hydrogen bond jump, respectively. They are explicitly given below:

$$\epsilon_C = 0.6 \tag{4}$$

$$\epsilon_S(j) = 0.5\epsilon_C \exp[-1.7(R_j - 1.4)] \tag{5}$$

$$\epsilon_H(k) = \epsilon_C{}^2 \exp[-1.7(R_k - 2.8)] \tag{6}$$

The distances are in angstroms. If there are several pathways that have comparable $H_{DA}$ values, those must be summed up to obtain total matrix elements:

$$H_{DA}(\text{total}) = \sum_I H_{DA}(I) \tag{7}$$

In the present case, the tunneling pathways were searched on each mutant with a bound Bi−Py molecule. The positions of the pyrenyl group, polypeptide chains, and the *p*-nitrophenyl group were taken from the computer-predicted conformation (Figure 8). In the calculation, the contribution of the polypeptide chains that belong to other subunits is also taken into consideration. Since the Bi−Py molecule is noncovalently bound to the protein, no direct through-bond pathway is possible and, as

(21) Baggott, J. E.; Philling, M. J. *J. Chem. Soc., Faraday Trans. 1* **1983**, *79*, 221.

(22) Personal communication from Professor Masashi Okada, Department of Chemistry, Faculty of Engineering Science, Osaka University, Osaka, Japan.

(23) Murakami, H.; Hohsaka, T.; Ashizuka, Y.; Sisido, M. In preparation.

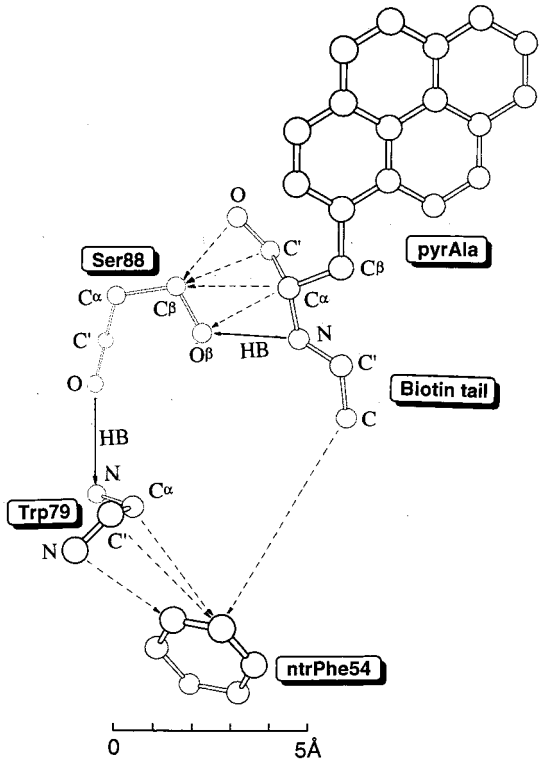


**Figure 12.** Major ET pathways found for ntrPhe54−streptavidin bound with a Bi−Py molecule.

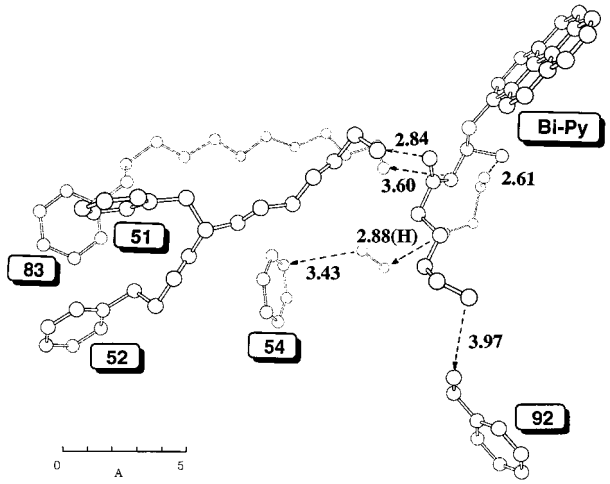


**Figure 13.** Optimum ET pathways from the pyrenyl group to the *p*-nitrophenyl groups at the 51st, 52nd, 54th, 83rd, and 92nd positions.

the result, a number of pathways that show comparable coupling matrix elements were found for each mutant. As a typical example, some of major pathways are illustrated for the 54th mutant in Figure 12. The optimum pathways for the 51st, 52nd, 54th, 83rd, and 92nd mutants are shown in Figure 13.

The coupling matrix elements $H_{DA}(I)$ for different pathways were summed, and the total matrix element $H_{DA}$(total) was obtained.[24] The total coupling matrix element may be expressed in terms of a nonintegral number ($n$) of $\sigma$ bonds that gives the same $H_{DA}$(total) value:

$$H_{DA}(\text{total}) = (\epsilon_C)^n = (0.6)^n \qquad (8)$$

If one takes 1.4 Å as the standard bond length for a $\sigma$ bond, the equivalent number of $\sigma$ bonds may be converted to an equivalent donor−acceptor $\sigma$ distance $\sigma_L$ that gives the same $H_{DA}$(total) value.

$$\sigma_L = 1.4n \qquad (9)$$

The $\sigma_L$ distances for the optimum ET pathway and those for the sum of the possible pathways are listed in Table 1. The observed ET rates were plotted against the $\sigma_L$ distance for the sum of the possible pathways in Figure 14. The solid line represents the expected distance dependence with $k_{ET0} = 10^{13}$ $s^{-1}$ at $\sigma_L = 3$ Å and $\beta_\sigma = 0.73$ Å$^{-1}$.

The points for the 65th, 117th, and 84th mutants are largely deviated from the expected distance dependence. To find the reason for this discrepancy, the optimum ET pathways for the three mutants are illustrated in Figure 15. In the cases of the 65th and 117th mutants, the pyrenyl group and the nitrophenyl group on the fourth and third subunits, respectively, are separated by a wide space. In these cases the fast ET observed experimentally may be explained either in terms of the thermal fluctuations of the fourth and third subunits with respect to the first subunit or in terms of the ET through electronic states of solvent molecules that are present in the intervening spaces. In the case of the 84th mutant, the through-bond ET is possible only through a long detour of the polypeptide chain. The ET accompanied by the fluctuations of the polypeptide chain or

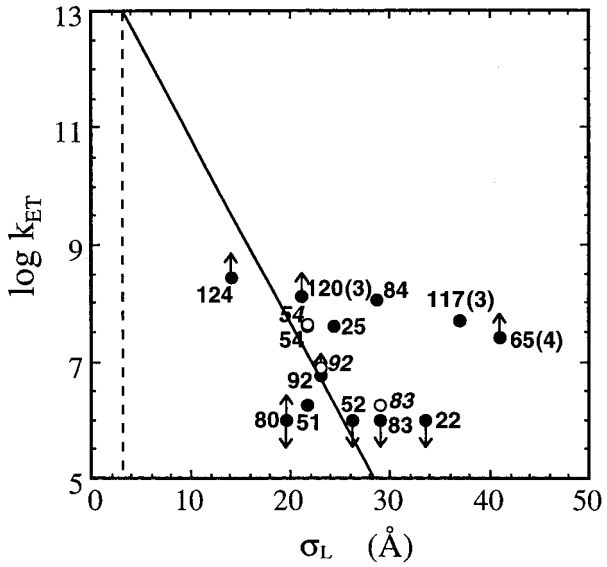


**Figure 14.** The observed ET rate constants in the ntrPhe−streptavidins plotted against the equivalent $\sigma$ distances for the sum of the possible ET pathways.

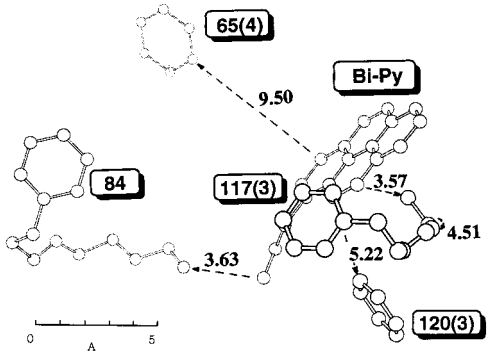


**Figure 15.** The ET pathways from the pyrenyl group of the Bi−Py molecule to the *p*-nitrophenyl group at the 65th position of the fourth subunit, the 84th position of the first subunit, the 117th position of the third subunit, and the 120th position of the third subunit.

(24) Mataga, N.; Kubota, T. *Molecular Interactions and Electronic Spectra*; Marcel Dekker: New York, 1970; Chapter 1.

the ET through solvent molecules may explain the faster rate than expected. The thermal fluctuations have been suggested from the nonexponential fluorescence decay curves as discussed above. For other mutants in which the ET may be mediated through the polypeptide chain and the biotin molecule, the deviation from the expected dependence is smaller.

It is therefore concluded that the ET rates for the singlet excited pyrenyl group to a *p*-nitrophenyl group in streptavidin are compatible with those of other proteins carrying metal complexes, except for the cases where ET occurs through a long space.

## Conclusion

It is concluded from this study that a single ntrPhe unit is successfully incorporated into specific positions of streptavidin. The positions and orientations of the *p*-nitrophenyl groups that were predicted from the molecular mechanics calculations were consistent with the ET rates from the excited pyrenyl group to the *p*-nitrophenyl group. The analysis of the ET rates on the basis of the tunneling pathway model indicated that the ETs across different subunits or those through a long detour of polypeptide chain are faster than the rates expected for direct through-space ET.

**Acknowledgment.** We thank professor Shigeyuki Yokoyama, University of Tokyo, for introducing to us the technique of *in vitro* biosynthesis. This research has been conducted with a Grant-in-Aid for Scientific Research from the Ministry of Education, Science, Sports, and Culture (06403034).

**Supporting Information Available:** The total sequences of DNAs that encode various mutants of streptavidin (1 page, print/PDF). See any current masthead page for ordering information and Web access instructions.

JA971890U